



Low nitrous oxide production through nitrifier-denitrification in intermittent-feed high-rate nitrification reactors

Su, Qingxian; Ma, Chun; Domingo-Felez, Carlos; Kiil, Anne Sofie; Thamdrup, Bo; Jensen, Marlene Mark; Smets, Barth F.

Published in:
Water Research

Link to article, DOI:
[10.1016/j.watres.2017.06.067](https://doi.org/10.1016/j.watres.2017.06.067)

Publication date:
2017

Document Version
Peer reviewed version

[Link back to DTU Orbit](#)

Citation (APA):
Su, Q., Ma, C., Domingo-Felez, C., Kiil, A. S., Thamdrup, B., Jensen, M. M., & Smets, B. F. (2017). Low nitrous oxide production through nitrifier-denitrification in intermittent-feed high-rate nitrification reactors. *Water Research*, 123, 429-438. <https://doi.org/10.1016/j.watres.2017.06.067>

General rights

Copyright and moral rights for the publications made accessible in the public portal are retained by the authors and/or other copyright owners and it is a condition of accessing publications that users recognise and abide by the legal requirements associated with these rights.

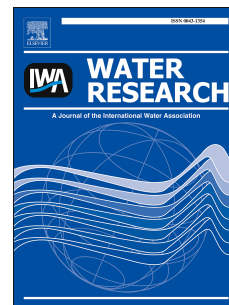
- Users may download and print one copy of any publication from the public portal for the purpose of private study or research.
- You may not further distribute the material or use it for any profit-making activity or commercial gain
- You may freely distribute the URL identifying the publication in the public portal

If you believe that this document breaches copyright please contact us providing details, and we will remove access to the work immediately and investigate your claim.

Accepted Manuscript

Low nitrous oxide production through nitrifier-denitrification in intermittent-feed high-rate nitritation reactors

Qingxian Su, Chun Ma, Carlos Domingo-Félez, Anne Sofie Kiil, Bo Thamdrup, Marlene Mark Jensen, Barth F. Smets



PII: S0043-1354(17)30528-6

DOI: [10.1016/j.watres.2017.06.067](https://doi.org/10.1016/j.watres.2017.06.067)

Reference: WR 13022

To appear in: *Water Research*

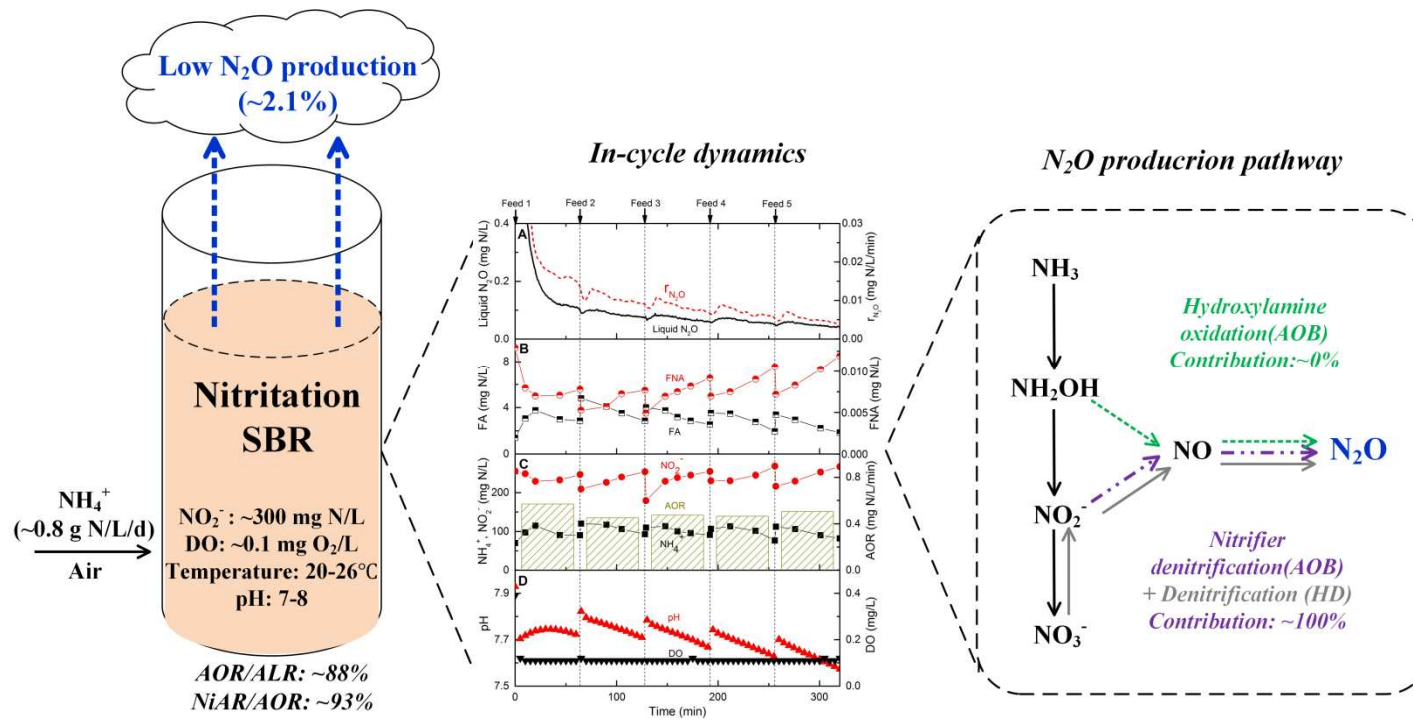
Received Date: 7 February 2017

Revised Date: 24 May 2017

Accepted Date: 19 June 2017

Please cite this article as: Su, Q., Ma, C., Domingo-Félez, C., Kiil, A.S., Thamdrup, B., Jensen, M.M., Smets, B.F., Low nitrous oxide production through nitrifier-denitrification in intermittent-feed high-rate nitritation reactors, *Water Research* (2017), doi: 10.1016/j.watres.2017.06.067.

This is a PDF file of an unedited manuscript that has been accepted for publication. As a service to our customers we are providing this early version of the manuscript. The manuscript will undergo copyediting, typesetting, and review of the resulting proof before it is published in its final form. Please note that during the production process errors may be discovered which could affect the content, and all legal disclaimers that apply to the journal pertain.



**Low nitrous oxide production through nitrifier-denitrification in
intermittent-feed high-rate nitrification reactors**

Qingxian Su ^a, Chun Ma ^b, Carlos Domingo-Félez ^a, Anne Sofie Kiil ^a, Bo Thamdrup ^b, Marlene
Mark Jensen ^{a*}, Barth F. Smets ^a

^a *Department of Environmental Engineering, Technical University of Denmark, 2800 Lyngby,
Denmark*

^b *Nordic Center for Earth Evolution and Institute of Biology, University of Southern Denmark, 5230
Odense M, Denmark*

* *Corresponding author.*

E-mail address: mmaj@env.dtu.dk

Abstract

Nitrous oxide (N₂O) production from autotrophic nitrogen conversion processes, especially nitrification systems, can be significant, requires understanding and calls for mitigation. In this study, the rates and pathways of N₂O production were quantified in two lab-scale sequencing batch reactors operated with intermittent feeding and demonstrating long-term and high-rate nitrification. The resulting reactor biomass was highly enriched in ammonia-oxidizing bacteria, and converted $\sim 93 \pm 14\%$ of the oxidized ammonium to nitrite. The low DO set-point combined with intermittent feeding was sufficient to maintain high nitrification efficiency and high nitrification rates at 20-26 °C over a period of ~ 300 days. Even at the high nitrification efficiencies, net N₂O production was low ($\sim 2\%$ of the oxidized ammonium). Net N₂O production rates transiently increased with a rise in pH after each feeding, suggesting a potential effect of pH on N₂O production. In situ application of ¹⁵N labeled substrates revealed nitrifier denitrification as the dominant pathway of N₂O production. Our study highlights operational conditions that minimize N₂O emission from two-stage autotrophic nitrogen removal systems.

Keywords: Nitrous oxide; Nitrification; Ammonia-oxidizing bacteria; Intermittent feeding; pH; Nitrifier denitrification

1. Introduction

Autotrophic nitrogen removal by combined partial nitrification (PN, aerobic ammonium (NH_4^+) oxidation to nitrite (NO_2^-)) and anammox (anaerobic NH_4^+ oxidation with NO_2^- to dinitrogen gas (N_2)) is being implemented as an energy and resource-efficient process compared to traditional nitrification and heterotrophic denitrification process (Siegrist et al., 2008; Wett et al., 2013). Autotrophic nitrogen removal can be achieved either in one- or two-stage systems. Although the two-stage process requires higher investment costs related to the construction, this configuration allows for coordination and optimization of the individual conversion stages (Desloover et al., 2011). The PN-anammox process offers a promising alternative for nitrogen removal that meets both lower energy consumption, mainly due to lower aeration need, and lower carbon footprint emission without requirement for external carbon addition (Kartal et al., 2010). Nitrification can be achieved by manipulating operation parameters, such as low dissolved oxygen (DO) and high NH_4^+ loadings, that are favorable for ammonia-oxidizing bacteria (AOB) over nitrite-oxidizing bacteria (NOB) (Blackburne et al., 2008; Vadivelu et al., 2007). However, low DO and high NH_4^+ as well as high accumulation of NO_2^- produced by AOB in two-stage systems may promote accumulation and emission of nitrous oxide (N_2O) (Kampschreur et al., 2008; Kim et al., 2010; Mampaey et al., 2016; Peng et al., 2015, 2014; Tallec et al., 2006).

The ongoing accumulation of N_2O in the atmosphere (~0.3% per year) is of great concern because it contributes to global warming (N_2O has a ca. 300 times higher global warming potential than CO_2) and the destruction of stratospheric ozone (IPCC, 2013; Stokal and Kroeze, 2014). Indeed, documented N_2O emissions of up to 17% of the NH_4^+ oxidized from both lab-scale and full-scale PN reactors have been higher compared to measurements from conventional nitrification-denitrification processes (Desloover et al., 2011; Gao et al., 2016; Kong et al., 2013; Lv et al., 2016; Mampaey et al., 2016). The variation in N_2O emissions might be explained by the different

responses of N_2O production and consumption pathways to different operation strategies (e.g. feeding and aeration pattern) and parameters (e.g. NH_4^+ , NO_2^- , DO and pH) (Burgess et al., 2002; Domingo-Félez et al., 2014; Law et al., 2011; Rathnayake et al., 2015; Schneider et al., 2014).

There are two main pathways involved in N_2O produced by AOB: (a) the reduction of NO_2^- to N_2O via nitric oxide (NO), known as nitrifier denitrification (ND) (Ishii et al., 2014; Kim et al., 2010; Wrage et al., 2001) and (b) N_2O as a side product during incomplete oxidation of hydroxylamine (NH_2OH) to NO_2^- (Law et al., 2012; Poughon et al., 2001; Tallec et al., 2006), known as hydroxylamine oxidation. Furthermore, denitrifying bacteria can be as important as AOB in the production of N_2O under very low C/N conditions (Domingo-Félez et al., 2017). During heterotrophic denitrification (HD), N_2O is an obligate intermediate and is produced during incomplete denitrification. The exact biological pathways and environmental controls of N_2O production in two-staged autotrophic nitrogen removal systems still remains to be quantified (Ishii et al., 2014; Law et al., 2012; Terada et al., 2017). A better quantitative understanding of the mechanisms for N_2O production is crucial to develop novel strategies or new designs to mitigate N_2O .

The principle goal of this study was to investigate N_2O dynamics and determine N_2O production pathways in two intermittently-fed lab-scale sequencing batch reactors (SBRs) with high nitrification performance. This was achieved by N_2O online measurements and *in situ* applications of ^{15}N labeled NH_4^+ or NO_2^- followed by monitoring of ^{15}N labeled and unlabeled products. In addition, the nitrification performance was assessed during the ~300 days of operation.

76 2. Materials and methods

77 2.1. Setup and operation of sequencing batch reactors (SBRs)

78 2.1.1 Reactor description and operation

79 Two SBRs (R1 and R2) with a working volume of 5L were used (Fig. S1, Support information). Air
80 supply was introduced by a bubble air diffuser and continuous mixing was provided with a
81 magnetic stirrer during the reaction and feeding phase. Air supply, mixing, and actuation of pumps
82 for fill and discharge were controlled by a programmable power strip EG-PM2-LAN (Gembird
83 Software Ltd., Almere, Netherlands).

84 R1 and R2 were operated as duplicates for 121 days, stopped for 170 days, where the biomass was
85 stored separately at 4 °C, and restarted for another 172 days. The operation period can be divided
86 into two phases: phase 1 (day 0–121) and phase 2 (day 291–463). The NH_4^+ and oxygen loading
87 were the two manipulative variables to sustain a low NOB/AOB activity. To recover biomass
88 activity after storage and maintain high NO_2^- accumulation, excess NH_4^+ and oxygen limitation
89 were set by stepwise increasing the ammonium loading rate (ALR) and air flow rate from 0.29 to
90 0.79 g N/L/d and 0.2 to 0.55 L/min, respectively (Table S1).

91 A 6-h working cycle was applied over the entire experiment. One cycle consisted of 320 min
92 reaction phase including five consecutive intervals of 1 minute feeding followed by a 63 minutes
93 inter-feed period, 30 min settling phase, 5 min decanting phase and 5 min idle phase. The
94 volumetric exchange ratio (VER) was 50%, resulting in a hydraulic retention time (HRT) of 12h.
95 The sludge retention time (SRT) was controlled at 20 days by wasting sludge at the end of reaction
96 phase. The reactors were operated at room temperature (20–26 °C) and without pH control.

2.1.2. Seed sludge and synthetic wastewater

The seeding sludge, originated from the return activated sludge stream at Mølleåværket WWTP (Lyngby, Denmark), was pre-cultivated and then inoculated into two SBRs.

Ammonium bicarbonate (NH_4HCO_3) was the only nitrogen source in the synthetic wastewater while NH_4HCO_3 and sodium bicarbonate (NaHCO_3) provided the inorganic carbon. The composition of trace chemicals (van de Graaf et al., 1996) was: 169.7 mg/L KH_2PO_4 , 751.1 mg/L $\text{MgSO}_4 \cdot 7\text{H}_2\text{O}$, 451.6 mg/L $\text{CaCl}_2 \cdot 2\text{H}_2\text{O}$, 5 mg/L EDTA, 5 mg/L $\text{FeSO}_4 \cdot 7\text{H}_2\text{O}$ and trace element solution of 1mL/L. The trace element solution contained 0.43 mg/L $\text{ZnSO}_4 \cdot 7\text{H}_2\text{O}$, 0.24mg/L $\text{CoCl}_2 \cdot 6\text{H}_2\text{O}$, 0.99mg/L $\text{MnCl}_2 \cdot 4\text{H}_2\text{O}$, 0.25mg/L $\text{CuSO}_4 \cdot 5\text{H}_2\text{O}$, 0.22mg/L $\text{NaMoO}_4 \cdot 2\text{H}_2\text{O}$, 0.19mg/L $\text{NiCl}_2 \cdot 6\text{H}_2\text{O}$ and 0.21mg/L $\text{NaSeO}_4 \cdot 10\text{H}_2\text{O}$.

2.2. N_2O measurement

Liquid phase N_2O was analyzed by a N_2O -R Clark-type microsensor (UNISENSE A/S, Århus, Denmark) and data was logged every 30s. Off-gas N_2O concentration was measured during phase 2 and logged on a minute basis (Teledyne API, San Diego, USA) to compare liquid and off-gas N_2O dynamics. As the reactors were not completely gas-tight during the periodic off-gas N_2O measurements, the liquid phase N_2O concentrations were used for the quantification of N_2O emission rates.

Net N_2O production and emission rates were calculated from the following equations:

$$\text{Instantaneous net } \text{N}_2\text{O} \text{ production rate, } r_{\text{N}_2\text{O}_i} = \frac{\Delta \text{N}_2\text{O}_i}{\Delta t} + k_L a_{\text{N}_2\text{O}_i} \cdot \text{N}_2\text{O}_i \quad \text{Eq. 1}$$

$$\text{Daily averaged net } \text{N}_2\text{O} \text{ production rate, } R_{\text{N}_2\text{O}} = \sum (r_{\text{N}_2\text{O}_i} \cdot \Delta t) \times 4 \frac{\text{cycle}}{\text{day}} \quad \text{Eq. 2}$$

Where $r_{\text{N}_2\text{O}_i}$ is the instantaneous net N_2O production rate at time i , $\frac{\Delta \text{N}_2\text{O}_i}{\Delta t}$ is the differential term of liquid concentration at time i , and $k_L a_{\text{N}_2\text{O}_i} \cdot \text{N}_2\text{O}_i$ is the stripping rate at time i , which equals the

emission rate. The N_2O volumetric mass transfer coefficient ($k_{\text{LaN}_2\text{O}}$) was determined experimentally at different volume/flow rates scenarios (Domingo-Félez et al., 2014) (Table S2). The net N_2O produced per NH_4^+ oxidized ($\Delta\text{N}_2\text{O}/\Delta\text{NH}_4^+$, %) and the specific net N_2O production rate (N_2OR , mg N/g VSS/d) were calculated from the daily averaged net N_2O production rate (Eq. 2).

2.3. DNA extraction and qPCR

Biomass samples were collected periodically from SBRs and centrifuged at 10,000 rpm for 5 min. Pellets were stored at -80°C until DNA extraction. DNA was extracted by FastDNATM SPIN Kit for Soil (MP Biomedicals, Solon, OH, USA), according to the manufacturer's instructions. The quantity and quality of the extracted DNA was measured and checked by its 260/280 ratio with a NanoDrop (ThermoFisher Scientific, Rockwood, TN, USA), and was stored at -20°C until further processing within a couple of weeks. qPCR was carried out on all the extracted DNA samples to determine the relative abundance of ammonia-oxidizing bacteria (AOB), nitrite-oxidizing bacteria (*Nitrobacter* NOB, *Nitrospira* NOB), anammox (AnAOB) and denitrifying bacteria, based on appropriate 16S rRNA targets and functional genes. Details on the procedure can be found in Terada et al. (2010). Primers and conditions used in various genes detection are listed in Table S3. All samples, including control reactions without template DNAs, were measured in duplicates.

2.4. ^{15}N additions and analysis

A ^{15}N experiment was designed to identify the microbial sources of N_2O production during operation of the nitrification SBRs (day 106 to 111). The ^{15}N -labeled nitrogen compounds ($>98\%$ ^{15}N ; Sigma-Aldrich) were added together with the second feed during the same cycle on different days (Table S4).

141 The resulting ^{15}N mole fractions of the nitrogen pools was 17-18% for $^{15}\text{NH}_4^+$ and 11-13 % for
 142 $^{15}\text{NO}_2^-$, as determined from the isotopic ^{15}N and total concentrations after additions. Reactor liquid
 143 (12 ml) was sampled every 10 minutes after tracer additions until the fourth feed of the cycle. For
 144 isotopic analysis of N_2O and N_2 , 3-mL and 6-mL Exetainer vials, respectively, prefilled with 100 μL
 145 of 50% (w/v) ZnCl_2 to stop microbial activity, were filled completely and immediately screw-
 146 capped with butyl rubber septa. Previous experiments had shown that ZnCl_2 efficiently quenched N
 147 transformations in this biomass (data not shown). The rest of the sample was filtered (0.22 μm) and
 148 frozen immediately for later analyses of nutrients and isotopic composition of NH_4^+ , NO_2^- and
 149 nitrate (NO_3^-).

150 Just before isotopic analysis of N_2O and N_2 , 1 and 1.5 ml of water was removed with a syringe and
 151 needle through the septum of the 3-mL and 6-mL Exetainer vials, respectively, while replacing the
 152 volumes with helium. The isotopic composition and concentration of N_2O and N_2 were determined
 153 using a gas chromatograph-isotope ratio mass spectrometer (Thermo Electron, Delta V advantage
 154 system) by injecting 1-mL and 200- μL samples of headspace directly from the Exetainer vials
 155 (Dalsgaard et al., 2012). The N-isotopic composition of NH_4^+ was analyzed after conversion to N_2
 156 with hypobromite (Warembourg, 1993). $^{15}\text{NO}_2^-$ was converted to N_2 with sulfamic acid (Füssel et
 157 al., 2012), while $^{15}\text{NO}_3^-$ was analyzed, after removal of any $^{15}\text{NO}_2^-$ with sulfamic acid, by cadmium
 158 reduction followed by conversion of the NO_2^- product to N_2 with sulfamic acid (McIlvin and
 159 Altabet, 2005).

160 Rates of ^{15}N -labeled N_2O and N_2 production were calculated from the measured excess
 161 concentrations of $^{14}\text{N}^{15}\text{NO}$, $^{15}\text{N}^{15}\text{NO}$, $^{14}\text{N}^{15}\text{N}$, and $^{15}\text{N}^{15}\text{N}$ and the k_{La} for N_2O and N_2 , respectively,
 162 similar to the calculations for bulk net N_2O production rate described above.

163 The total conversion of NH_4^+ and NO_2^- to the gaseous products, irrespective of the pathway, was
 164 determined by division of the rate of ^{15}N -labeled gas production ($^{15}\text{N}-\text{N}_2\text{O} = ^{14}\text{N}^{15}\text{NO} + 2 \times$

$^{15}\text{N}^{15}\text{NO}$; $^{15}\text{N}-\text{N}_2 = ^{14}\text{N}^{15}\text{N} + 2 \times ^{15}\text{N}^{15}\text{N}$) by the labeling fraction F of the substrate ($F_A = [^{15}\text{NH}_4^+] \times [\text{NH}_4^+]^{-1}$ and $F_N = [^{15}\text{NO}_2^-] \times [\text{NO}_2^-]^{-1}$), e.g.:

$$\text{Rate}(\text{NH}_4^+ \rightarrow \text{N}_2\text{O}) = \text{Rate}(^{15}\text{NH}_4^+ \rightarrow ^{15}\text{N}-\text{N}_2\text{O}) \times F_A^{-1} \quad \text{Eq. 3}$$

Production of N_2O through denitrification in the $^{15}\text{NO}_2^-$ experiments was calculated in two ways (Eq. 4 and 5), both based on the principle of random nitrogen isotope pairing (Nielsen, 1992) and resting on the assumption that denitrification is the only source of double-labeled products with $^{15}\text{NO}_2^-$. Here, Eq. 4 represents a rate based on NO_2^- in the bulk liquid only, with a known F_N , and Eq. 5 represents a situation where F_N at the site of reaction may differ from that in the bulk liquid and is instead estimated from the ratio of $^{15}\text{N}^{15}\text{NO}$ production to $^{14}\text{N}^{15}\text{NO}$ production, R_{46} :

$$\text{Denitrification}_{\text{N}_2\text{O}, \text{ bulk}} = \text{Rate}(^{15}\text{N}^{15}\text{NO}) \times F_A^{-2} \quad \text{Eq. 4}$$

$$\text{Denitrification}_{\text{N}_2\text{O}, \text{ coupled}} = \text{Rate}(^{15}\text{N}^{15}\text{NO}) \times (2R_{46} \times [1 + 2R_{46}]^{-1})^{-2} \quad \text{Eq. 5}$$

2.5. Analytical methods

Liquid effluent samples were filtered through 0.45 μm pore size filters before nitrogen species analysis. NH_4^+ and NO_2^- were measured colorimetrically according to Bower and Holm-Hansen (1980) and Grasshoff (1999) respectively, while NO_3^- was analyzed by autoanalyzer (AutoAnalyzer 3, SEAL Analytical) with the cadmium-reduction method (Armstrong et al., 1967; Grasshoff, 1999). Reactor performance was described by computing the observed ammonium oxidizing rate (AOR, mg N/L/d), nitrite accumulation rate (NiAR, mg N/L/d), nitrate accumulation rate (NaAR, mg N/L/d) (Eq. S2-4). Free ammonia (FA) and free nitrous acid (FNA) concentration were calculated following Anthonisen et al. (1976) (Eq. S5-6). Mixed liquid suspended solids (MLSS) and mixed liquor volatile suspended solids (MLVSS) were measured following standard methods (APHA, 1998). DO and pH were monitored continuously (WTW GmbH, Weilheim, Germany).

3. Results

3.1. Reactor performance

3.1.1. Nitritation performance

Both reactors were operated towards high nitritation performance, and displayed stable NH_4^+ removal at the end of phase 1 (day 78–121) and phase 2 (day 291–463) (Fig. 1). At the loading of 0.57 g N/L/d at the end of phase 1, the average ammonium oxidizing efficiency (AOR/ALR) was $83 \pm 12\%$ (average \pm standard deviation) and $90 \pm 11\%$ for R1 and R2, respectively. With stepwise increases in loading from 0.29 to 0.79 g N/L/d during phase 2, the average AOR/ALR remained relatively stable at $86 \pm 11\%$ (R1) and $88 \pm 8\%$ (R2) during phase 2, except for a $\sim 19\%$ decline in the final days of the reactors (Fig. 1). There was high NO_2^- accumulation at the end of phase 1 and throughout phase 2, maintaining average nitrite accumulation efficiency (NiAR/AOR) of $92 \pm 17\%$ and $93 \pm 14\%$ in R1 and R2, respectively. NO_3^- accumulated at low concentrations throughout the whole operation period (Fig. 1). Nitrate accumulation efficiency (NaAR/AOR) in R1 and R2 was maintained at $11 \pm 9\%$ and $14 \pm 8\%$ respectively, indicating low NOB activity.

3.1.2. In-cycle dynamics of nitrogen species, DO and pH

The reactors were operated with five intermittent feedings, without on-line pH control, and pH slightly decreased from 7.85 to 7.55 within a cycle (Fig. 2). pH transiently increased after each feeding due to the bicarbonate and phosphate content of the influent. During the inter-feed periods, pH decreased due to proton release during nitritation. DO concentrations were close to the limit of quantification of 0.1 mg/L during the reaction phase (Fig. 2). NH_4^+ concentration increased at each feeding while NO_2^- concentration decreased due to dilution. Concentrations of FA and FNA varied between 1.39 to 4.79 mg N/L and 0.005 to 0.013 mg N/L, respectively, reflecting the changes in NH_4^+ and NO_2^- concentrations at different pH (Fig. 2). During the inter-feed periods, AOR was relatively constant with an average value of 0.49 ± 0.04 mg N/L/min (Fig. 2).

211 3.2. N₂O production

212 3.2.1. Overall N₂O production

213 During the end of phase 1, the average net N₂O produced per NH₄⁺ oxidized ($\Delta\text{N}_2\text{O}/\Delta\text{NH}_4^+$) in R1
 214 and R2 was $0.6 \pm 0.2\%$ and $0.8 \pm 0.3\%$ respectively; while it was $2.0 \pm 1.0\%$ and $2.1 \pm 0.7\%$ during
 215 phase 2 (Table 1). The liquid N₂O concentrations as well as $\Delta\text{N}_2\text{O}/\Delta\text{NH}_4^+$ increased during phase 2
 216 (Fig. 3 and Table 1) in two reactors. The differences in the specific net N₂O production rate (N₂OR)
 217 between the two reactors were likely due to the differences in MLVSS concentrations. Furthermore,
 218 each inter-feed period did not contribute equally to the total N₂O production of a cycle. N₂O gas
 219 escaping after feed 1, ranging between 23 to 41% in both reactors during two phases, was
 220 considerable higher compared to the emissions following the other feeds (Table 1).

221 3.2.2. N₂O dynamics during intermittent feedings

222 The patterns of liquid N₂O concentration profiles over the reaction phase were very reproducible
 223 during the whole period for both reactors (Fig. 2 and 3). In-cycle N₂O profiles had the following
 224 pattern: after the settling phase from the previous cycle, an initial maximum in N₂O concentration
 225 occurred when the first feed initiated, after which the concentration declined until the next feeding;
 226 another four smaller peaks in N₂O concentration were observed in the subsequent feedings. N₂O
 227 concentration reached minimum values in the inter-feed periods but with concentrations higher than
 228 the detection limit of the sensor. Thus, based on liquid N₂O concentrations there was always a
 229 positive net production of N₂O in both reactors, with rates ($r_{\text{N}_2\text{O}_i}$) increasing after each feeding and
 230 decreasing during inter-feed periods (Fig. 3). Off-gas N₂O profiles followed the same trends during
 231 the reaction phase.

3.3. Microbial community composition dynamics

The optimization of the reactor operation during phase 1 caused clear shifts in the microbial community, as indicated by qPCR analysis using relevant primers (Fig. 4). The microbial community composition was similar between the two reactors. The relative abundance of *Nitrobacter* spp. decreased at the end of phase 1, where *Nitrobacter* spp. was 2–3 orders of magnitude higher than *Nitrospira* spp. Both *Nitrobacter* spp. and *Nitrospira* spp remained very low throughout phase 2. Both 16S rRNA gene and *nxrA* targeted NOB quantifications were consistent in phase 2 (Fig. 4 and S2). The overall reduction in NOB relative abundance was mirrored by a significant increase in AOB numbers, as reflected by both the 16S rRNA gene and *amoA* targeted quantifications (Fig. 4 and S2). AOB remained dominant in both reactors throughout the operation period. The relative abundance of AnAOB, based on 16S rRNA gene quantification, was low but existent ($0.96 \pm 0.01\%$ and $1.94 \pm 0.01\%$ in R1 and R2, respectively). The ratio of *nirS* plus *nirK* over *nosZ*-targeted quantifications was far above 1 (Fig. S2).

3.4. N₂O production pathway

In incubations with ¹⁵N-labeled substrates, the label was transferred to both N₂O and N₂ within 2–3 minutes of addition, irrespective of whether ¹⁵N was added as ¹⁵NO₂[−] or ¹⁵NH₄⁺ (Fig. 5). The dynamics of ¹⁵N-N₂O mirrored those of bulk N₂O, and N₂O was the dominating product in ¹⁵NO₂[−] incubations accounting for 57–58% of the labeled N₂O + N₂ in both feedings, while it only accounted for 17–23% with ¹⁵NH₄⁺. The production of N₂ was also highly dynamic, showing an even steeper rise after feeding than for N₂O. The production of ¹⁵N-N₂O from ¹⁵NO₂[−] corresponded to a total conversion of NO₂[−] to N₂O of 5.7–9.9 μg N/g VSS/min, which was not significantly different from the total net N₂O production (Table 2), implying that NO₂[−] was the main source of N₂O in the incubations.

255 There was no detectable production of $^{15}\text{NH}_4^+$ in the incubations with $^{15}\text{NO}_2^-$ (data not shown),
 256 which implies that all $^{15}\text{N-N}_2\text{O}$ and $^{15}\text{N-N}_2$ in these incubations was formed exclusively through
 257 reductive pathways, i.e., not via dissimilatory nitrate/nitrite reduction to ammonium (DNRA) and
 258 subsequent oxidation of NH_4^+ .

259 Indeed, the relative production of $^{14}\text{N}^{15}\text{NO}$ and $^{15}\text{N}^{15}\text{NO}$ from $^{15}\text{NO}_2^-$ (Fig. 5) was close to that
 260 expected from denitrification with random isotope pairing (either heterotrophic or nitrifier
 261 denitrification). Thus, the production of N_2O through denitrification (calculated by Eq. 4)
 262 corresponded to 80% and 77% of total net N_2O production from NO_2^- (the NO_2^- -to- N_2O conversion
 263 rates calculated by Eq. 3) on average for feed 2 and 3, respectively (Table 2). The remaining 20–
 264 23% of NO_2^- -derived N_2O corresponds to a surplus of $^{14}\text{N}^{15}\text{NO}$ relative to the prediction from
 265 random isotope pairing from the bulk NO_2^- pool, and therefore indicates pairing of N from this pool
 266 with N from a second source of unlabeled N. The surplus of $^{14}\text{N}^{15}\text{NO}$ may arise if the labeling
 267 fraction of NO_2^- , F_N , in the immediate vicinity of the nitrite reductase enzymes is lower than the
 268 bulk F_N value used for the calculations (Eq. 4), e.g., because of dilution with unlabeled NO_2^- from
 269 nitrification maintained by diffusional gradients either intracellularly or within microaggregates. This
 270 is reflected in the N_2O production calculated by Eq. 5, which derives F_N at the site of NO_2^-
 271 reduction from the relative production of $^{14}\text{N}^{15}\text{NO}$ and $^{15}\text{N}^{15}\text{NO}$. Thus, assuming that all conversion
 272 of NO_2^- to N_2O occurred through a denitrification pathway, total N_2O production was calculated
 273 based on the relative production of $^{14}\text{N}^{15}\text{NO}$ and $^{15}\text{N}^{15}\text{NO}$ (Nielsen, 1992), yielding rates that
 274 exceeded the NO_2^- -to- N_2O conversion rates by 24–31% (Table 2).

275 The production of N_2O from NH_4^+ , determined in incubations with $^{15}\text{NH}_4^+$ showed very similar
 276 temporal dynamics as N_2O production from NO_2^- (Fig. 5). After the 2nd feed, the production from
 277 NH_4^+ corresponded, on average, to 42% of the production from NO_2^- (Table 2). This fraction
 278 increased to 58% after the 3rd feed, which is explained by the accumulation of $^{15}\text{NO}_2^-$ and the

279 resulting increasing contribution of $^{15}\text{N}_2\text{O}$ from denitrification, as also reflected in the higher
 280 concentrations of ^{15}N - N_2O reached after the 3rd feed relative to the 2nd (Fig. 5). The amount of ^{15}N -
 281 N_2O produced from $^{15}\text{NH}_4^+$ via nitrification, mixing of the formed $^{15}\text{NO}_2^-$ with the bulk NO_2^- pool,
 282 and subsequent denitrification, was estimated for each reactor based on the rates of N_2O production
 283 determined in the $^{15}\text{NO}_2^-$ incubations in the same reactor and the F_N values (data not shown) from
 284 the $^{15}\text{NH}_4^+$ incubations (Eq. 3). These calculations indicated that 25% and 49% of N_2O production
 285 determined with $^{15}\text{NH}_4^+$ occurred via bulk NO_2^- after feed 2 and 3, respectively. The $^{15}\text{NH}_4^+$ -based
 286 N_2O production that was not attributable to this route averaged $2.6 \mu\text{g N/g VSS/min}$ after both
 287 feedings, corresponding to 25% of the combined N_2O production detected with $^{15}\text{NO}_2^-$ and $^{15}\text{NH}_4^+$
 288 (Table 2), and the sum of this rate and the production of N_2O from NO_2^- matched the estimated N_2O
 289 production from denitrification closely (7.7 vs. $7.3 \mu\text{g N/g VSS/min}$ and 12.1 vs. $12.5 \mu\text{g N/g}$
 290 VSS/min for R1 and R2, respectively). The contribution of the hydroxylamine oxidation pathway to
 291 N_2O production did *not* increase immediately after the addition of NH_4^+ , as the production ratio
 292 between $^{15}\text{N}^{15}\text{NO}$ and $^{15}\text{N}^{14}\text{NO}$ did not change significantly over time after feed 2 and 3. Thus, the
 293 $^{15}\text{NO}_2^-$ and $^{15}\text{NH}_4^+$ in combination support a denitrification pathway as the main and possibly sole
 294 source of N_2O in this SBR system.

295 In the $^{15}\text{NO}_2^-$ incubations, the relative abundance of single and double-labeled N_2 ($^{14}\text{N}^{15}\text{N}$ and
 296 $^{15}\text{N}^{15}\text{N}$) differed markedly from that of N_2O , with $^{15}\text{N}^{15}\text{N}$ accounting for $\leq 0.5\%$ of the labeled N_2
 297 compared a contribution of $\sim 5\%$ from $^{15}\text{N}^{15}\text{NO}$ to labeled N_2O (Fig. 5). This pointed towards
 298 another N_2 source than denitrification. The total N_2 production rate from NO_2^- (Eq. 3) was 4.4 ± 0.9
 299 and $6.4 \pm 0.8 \mu\text{g N/g VSS/min}$ for R1 and R2, respectively. Substantially higher N_2 production rates
 300 were obtained for the $^{15}\text{NH}_4^+$ than with $^{15}\text{NO}_2^-$: 10.2 ± 3.5 and $21 \pm 0.8 \mu\text{g N/g VSS/min}$ for R1 and
 301 R2, respectively. Correction of these rates for ^{15}N - N_2 produced from the accumulating $^{15}\text{NO}_2^-$

(performed similarly as for the N_2O production rates from $^{15}\text{NH}_4^+$) only reduced these rates slightly to 9.4 ± 3.5 and 19.7 ± 1.5 $\mu\text{g N/g VSS/min}$, respectively.

4. Discussion

4.1. Mechanisms to achieve high and stable nitrification performance

Two SBRs were operated for approximately 300 days with high NO_2^- accumulation and no significant production of NO_3^- , which indicates that NOB were successfully outcompeted by AOB (Fig. 1). The suppression of NOB and enrichment of AOB was verified by an average AOB/NOB ratio of >200 at the end of phase 1 and during phase 2 (Fig. 4). Various parameters such as DO, FA, FNA, temperature and feeding strategy have been reported to affect the selective enrichment of AOB over NOB (Blackburne et al., 2008; Hellenga et al., 1998; Liu and Wang, 2014; Vadivelu et al., 2007; Yang et al., 2013).

Oxygen limitation is a critical factor to achieve and maintain high nitrification performance. AOB are postulated to outcompete NOB at low DO concentrations due to the higher oxygen affinity of AOB than NOB (Blackburne et al., 2008; Wiesmann, 1994). DO below 1.0 mg/L was previously reported to inhibit the growth of NOB and instead enhance the growth of AOB, resulting nitrite accumulation (Sinha and Annachhatre, 2007; Tokutomi, 2004). For instance, stable nitrite accumulation efficiency (NiAR/AOR) of 70% and 85% is achieved at DO of 0.1 mg/L and 0.5–1.0 mg/L, respectively (Gao et al., 2016; Guo et al., 2013). As the DO level in our two nitrification SBRs was ≤ 0.1 mg/L, oxygen limitation is an important factor for NOB inhibition at the end of phase 1 and throughout phase 2, where high nitrification efficiencies of $92 \pm 17\%$ (R1) and $93 \pm 14\%$ (R2) were maintained (Fig. 1).

Among other factors, FA and FNA are commonly selected as the key parameters to achieve high nitritation because of the different impacts on AOB and NOB (Anthonisen et al., 1976; Brockmann and Morgenroth, 2010; Vadivelu et al., 2007; Yamamoto et al., 2008). Many studies have reported FA and FNA concentrations that might inhibit NOB growth and trigger AOB proliferation; however, the critical values reported in these studies were variable (Anthonisen et al., 1976; Bae et al., 2001; Vadivelu et al., 2007). Regarding FA, NOB has been found to be inhibited at concentrations ranging from 0.1 to 1 mg N/L, while AOB was inhibited at 10-150 mg N/L (Anthonisen et al., 1976). This agrees with a recent study by Vadivelu and coworkers (2007), where NOB activity was totally inhibited by 6.0 mg N/L and AOB activity was unaffected at up to 16 mg N/L. The increase in FA concentration by a factor of ~5 from phase 1 I to phase 1 II and 2, where the FA concentration was 3.1 ± 0.8 mg N/L, could be the reason for a decrease in nitrate accumulation, especially in R1 (Fig. 1 and 2). However, FA did not fully inhibit the activity of NOB at any time in our study. Also, within the observed FA concentration, FA likely had no effect on the activity of AOB.

It has been reported that NOB activity was inhibited by FNA at concentrations between 0.02 and 0.2 mg N/L (Hellings et al., 1998; Vadivelu et al., 2007). Compared to these studies, FNA at 0.008 ± 0.002 mg NO_2^- -N/L was too low to have a negative effect on NOB activity (Fig. 2). Throughout the whole SBR operation period, AOR correlated positively with NO_2^- concentrations, reaching the maximum (0.8 g N/L/d) at 323 mg N/L (Fig. S3). Hence, no evidence of NO_2^- inhibition was obtained. The observed increase in AOR with increasing NO_2^- concentration agrees with a previous study with mixed microbial communities, showing high ammonium oxidation to NO_2^- (150–160 mg NO_2^- -N/h/g VSS) at NO_2^- concentrations up to 1000 mg N/L (Law et al., 2013). Nevertheless, the calculated FNA concentrations in this study (ca. 0.008 mg HNO_2^- -N/L) remain much below reported inhibitor concentrations (FNA of 0.1 mg/L) (Hiatt and Grady, 2008).

Temperature is another parameter that can affect the relative competitiveness of AOB over NOB. NOB were outcompeted by AOB at moderate temperatures (20-26 °C), resulting in high nitrification efficiency from day 78 onwards (Fig. 1). This finding contrasts with the general assumption of high temperatures (30-35 °C) are needed for selective removal of NOB over AOB (Hellenga et al., 1998; Yang et al., 2007).

It is often difficult to maintain stable nitrification over the long-term period even in successfully established nitrification systems (Bernet et al., 2001; Fux et al., 2004; Villaverde et al., 2000; Yang et al., 2013). For instance, Villaverde and coworkers (2000) obtained high NiAR/AOR of 65% in submerged nitrifying biofilters, however, after 6 months NOB became acclimated to high FA and NiAR/AOR decreased to 30%. Moreover, Bernet and coworkers (2001) observed a transition from stable nitrification in a two-stage PN-anammox process for more than 100 days to complete nitrification within 2 days caused by a transient increase of DO. Here, SBRs were operated for ~300 days with high nitrification efficiency and high AOB abundance accompanied by low NO_3^- accumulation and low NOB abundance. We speculate that using intermittent feeding together with low DO set-points successfully enabled long-term high nitrification performance in the two SBR reactors. While long-term high-rate nitrification has not been reported yet in intermittently fed SBRs, high nitrite accumulation (NiAR/AOR) of 85% and >95% was previously reported for 150 and 174 days, respectively, in step-feed A/O SBRs (Lemaire et al., 2008; Yang et al., 2007). Hence, low DO control and intermittent feeding appear key operational strategies to obtain continuous NOB suppression at suboptimal temperatures.

4.2. Low N_2O production

The net N_2O produced per NH_4^+ oxidized ($\Delta\text{N}_2\text{O}/\Delta\text{NH}_4^+$) and the specific net N_2O production rate (N_2OR) of the two nitrification SBRs were compared to previously reported values together with the identification of reactor types, operation strategies, performance and AOB presence (Table S5). The

372 average net N₂O production in phase 2 increased to $2.0 \pm 1.0\%$ and $2.1 \pm 0.7\%$ of the NH₄⁺ oxidized
 373 in R1 and R2, respectively, while the average specific net N₂O production rate was 8.4 ± 3.5 and
 374 10.2 ± 3.5 mg N/g VSS/d in R1 and R2, respectively (Table 1 and S5). The net N₂O production in
 375 both reactors corresponded well with the genetic potential for N₂O production, as the ratio of *nirS*
 376 plus *nirK* over *nosZ*-targeted genes was far above 1 (Fig. S2). The higher N₂O production in phase
 377 2 compared to phase 1 is puzzling as it cannot be explained by higher AOR (Table 1). We speculate
 378 that the long-term operation under elevated NO₂⁻ may have selected for new microbes with higher
 379 expression of the nitrifier-denitrification pathway or the cultured microbes adapted to higher NO₂⁻,
 380 resulting in higher expression of the pathway, and with that higher N₂O production. This theory,
 381 however, calls for deeper analysis of the microbial community than obtained with qPCR.

382 The N₂O production factors of ~2% are in the low range of previous reports for both lab-scale and
 383 full-scale PN systems, ranging between 1–17% (Table S5). Our study is the first study to measure
 384 low N₂O emissions at very high nitrification efficiencies. Low DO (0.35 mg/L) and high NO₂⁻
 385 conditions (10 – 50 mg N/L) boost N₂O production (Peng et al., 2015, 2014). Measured N₂O
 386 emissions are lower compared to other lab-scale PN SBRs operated under low DO and high NO₂⁻
 387 conditions (N₂O emissions of 17%) (Gao et al., 2016; Lv et al., 2016). With the intermittent feeding
 388 strategy at low DO, we force relatively low ammonia oxidation rates (Fig. 2, Table 1), which has
 389 previously been shown to decrease N₂O emissions from autotrophic nitrogen removal systems
 390 (Domingo-Félez et al., 2014; Law et al., 2011). Law and coworkers (2011) found that a decline in
 391 feeding rate from 1 L/2.5 min to 1 L/25 min during the reaction phase lead to a substantial reduction
 392 in N₂O production without affecting the nitrification performance. Instead of reducing the feeding rate,
 393 our nitrification reactors were operated with five intermittent feedings within a cycle. This step-feed
 394 strategy has previously been suggested as an effective optimization approach to reduce N₂O

emissions from SBRs (Mavrovas, 2014; Yang et al., 2009, 2013). Therefore, we postulate that intermittent feeding is the cause for the low N_2O emission from high-performance nitrification system.

4.3. Potential pH effect on in-cycle N_2O production dynamics

Distinctive N_2O production profiles were observed within the representative cycles (Fig. 2 and 3). The maximum net N_2O production and the subsequent decrease after the first feed has also been described in various studies (Ali et al., 2016; Itokawa et al., 2001; Kampschreur et al., 2008; Mampaey et al., 2016; Rodriguez-Caballero and Pijuan, 2013). Rodriguez-Caballero and Pijuan (2013) showed that 60% of the total N_2O production occurred during the settling phase in their lab-scale PN SBR, while 70% of the quantified N_2O emission was attributed to the anoxic N_2O formation in a full-scale PN SHARON reactor (Mampaey et al., 2016). Tentative liquid N_2O measurements indicated that N_2O accumulated during the non-aerated settling phase (data not shown). Denitrification might be responsible for this N_2O accumulation during the settling phase, which is then released at the onset of aeration (Itokawa et al., 2001). The genetic potential for N_2O production by denitrifiers was present through the high relative abundance of *nirS* (Fig. S2).

A potential effect of pH on N_2O production during the reaction phase was indicated by the transiently increase in net N_2O production rates with the rise in pH after each feeding pulse (Fig. 2 and 3). There was no obvious changes in DO, and although NH_4^+ and FA increased transiently after each feeding, FA was always in excess compared to the K_m value of 0.0075 mg/L for AOB, and therefore AOR remained unaffected (Fig. 2) (Hiatt and Grady, 2008). Thus, pH appears the only potential variable affecting in-cycle N_2O dynamics. Only few studies have been able to isolate the effect of pH on N_2O production from the variations in FA and FNA, and the reported effect of pH on N_2O production differ. In contrast to our results, Law and coworkers (2011) obtained highest N_2O and AOR at pH 8 in the investigated pH range of 6.0–8.5, independently from FA and FNA concentrations, suggesting that an increase in ammonium oxidation activity might promote N_2O

production. Oppositely, Rathnayake et al. (2015) observed highest N_2O emission at pH 7.5 in PN granules, although AOR was unchanged between pH 6.5 and 8.5. Further research is needed to resolve whether the pH effect on N_2O production is direct or indirect.

4.4. N_2O production pathway

The experiments with ^{15}N labeled substrates point to nitrifier denitrification as the dominant source of N_2O in the SBR nitrification systems. A denitrification-type process rather than a direct production of N_2O from ammonium oxidation via hydroxylamine was demonstrated by more than 3 times higher rates of N_2O production from NO_2^- than from NH_4^+ , when $^{15}\text{NH}_4^+$ -derived rates were corrected for accumulation of $^{15}\text{NO}_2^-$ (Table 2). Moreover, isotope pairing calculations showed that NO_2^- during its reduction to N_2O was mixed with nitrogen from an unlabeled source. In the nitrification-dominated system, NH_4^+ is the most obvious candidate, and indeed, the production rate of N_2O from NH_4^+ that did not go via bulk NO_2^- closely matched the difference between total and bulk NO_2^- -dependent denitrification. We therefore hypothesize that essentially all N_2O was produced through nitrifier-denitrification with part of the newly-formed NO_2^- shunted directly to reduction either intracellularly or within cellular aggregates before it could mix completely with NO_2^- in the bulk liquid. Alternatively, the combination of N from NH_4^+ and NO_2^- could occur at the level of NO if this compound is a free intermediate during ammonium oxidation (Stein, 2011). The ^{15}N -labeling technique in itself cannot distinguish nitrifier denitrification from heterotrophic denitrification. However, several pieces of evidence point to the former process. Firstly, the stimulation of N_2O production by each NH_4^+ feeding points to NH_4^+ dependence rather than heterotrophy. Secondly, there is no convincing evidence for heterotrophic N_2 production: (a) The rate of N_2O production exceeds the rate of N_2 production from NO_2^- whereas N_2O is generally a minor byproduct of heterotrophic denitrification (Betlach and Tiedje, 1981); (b) the dynamics of N_2 and N_2O production are out of phase with the peak in N_2 preceding that of N_2O , where the opposite

would be expected during heterotrophic denitrification (e.g., Jensen et al., 2009), and (c) the very low ratio of $^{15}\text{N}^{15}\text{N}$ to $^{14}\text{N}^{15}\text{N}$, differing markedly from the $^{15}\text{N}^{15}\text{NO}:$ $^{14}\text{N}^{15}\text{NO}$ ratio in N_2O , suggests that N_2 production from NO_2^- is mainly due to another process, possibly anammox.

The complete dominance of nitrifier-denitrification as source of N_2O is in general agreement with the understanding that this process is favored by low DO and high NO_2^- levels (e.g., Colliver and Stephenson, 2000; Kampschreur et al., 2008; Peng et al., 2015; Tallec et al., 2006). The high rates of N_2 production observed in the $^{15}\text{NH}_4^+$ incubations, relative to both N_2O production in the same experiment and to N_2 production with $^{15}\text{NO}_2^-$, suggests an involvement of anammox. Only a small part of the N_2 produced with $^{15}\text{NH}_4^+$ could be explained with oxidation to NO_2^- and subsequent reduction, which means that NH_4^+ appeared to be converted directly from NH_4^+ to N_2 . As N_2 production has not been documented in aerobic ammonium oxidizers, this suggests the involvement of anammox bacteria, which were indeed detected in the biomass (Fig. 4) in low abundance. As anammox represents a 1:1 pairing of N from NH_4^+ and NO_2^- , similar rates of N_2 production should, however, be obtained with additions of $^{15}\text{NH}_4^+$ and $^{15}\text{NO}_2^-$ (van de Graaf et al., 1995), whereas we observed ~2.5-fold higher production from $^{15}\text{NH}_4^+$ than from $^{15}\text{NO}_2^-$. Potential explanations for the imbalance in rates are either a close coupling of nitrification and anammox, which would require a physical association of anammox bacteria and ammonium oxidizers, or variation in anammox rates between the two series of experiments, which were conducted 5 days apart. The resolution of these issues is, however, beyond the scope of this study.

5. Conclusion

Two lab-scale intermittently-fed nitrification SBRs were operated to investigate N_2O dynamics and identify N_2O production pathways.

- High nitrification performance with $\sim 93 \pm 14\%$ of the oxidized NH_4^+ converted to NO_2^- was achieved in intermittently-fed SBRs at 20-26°C for ~ 300 days.
 - The averaged net N_2O production factor of $2.1 \pm 0.7\%$ is in the low range: Operation with intermittent feeding may be an effective approach to minimize N_2O emissions from nitrification systems.
 - Increased net N_2O production rate was observed with pH increase after each feeding. Further investigations are required to identify the exact mechanisms of the pH effect on enzymes, pathways and bacteria involved in N_2O production.
 - Nitrifier denitrification was the dominant source of N_2O .
- This study has demonstrated operational conditions (low dissolved oxygen and intermittent feeding) that achieve high-rate and long-term nitrification under normal temperature, which could enlarge the applicability of the nitrification process in WWTPs. The relatively low N_2O production at high nitrification efficiencies reduces the growing concern of N_2O production from autotrophic nitrogen processes in WWTPs. The identification of nitrifier denitrification as the main pathway of N_2O emissions will open up for more focused strategies to lower the N_2O footprint even more in nitrification systems.

Acknowledgements

The work has been funded in part by the China Scholarship Council, the Innovation Fund Denmark (IFD) (Project LaGas, File No. 0603-00523B) and The Danish Council for Independent Research Technology and Production Sciences (FTP) (Project N_2Oman , File No. 1335-00100B). The authors thank Lene Kirstejn Jensen for the assistance during qPCR measurements.

References

Ali, M., Rathnayake, R.M.L.D., Zhang, L., Ishii, S., Kindaichi, T., Satoh, H., Toyoda, S., Yoshida, N., Okabe, S., 2016.

- Source identification of nitrous oxide emission pathways from a single-stage nitrification-anammox granular reactor. *Water Res.* 102, 147–157.
- Anthonisen, A., Loehr, R., Prakasam, T., Srinath, E., 1976. Inhibition of Nitrification by Ammonia and Nitrous Acid. *J. Water Pollut. Control Fed.* 48, 835–852.
- APHA, 1998. *Standard Methods for the Examination of Water and Wastewater*, 20th ed. American Public Health Association, Washington, DC.
- Armstrong, F.A.J., Stearns, C.R., Strickland, J.D.H., 1967. The measurement of upwelling and subsequent biological process by means of the Technicon Autoanalyzer® and associated equipment. *Deep Sea Res. Oceanogr. Abstr.* 14, 381–389.
- Bae, W., Baek, S., Chung, J., Lee, Y., 2001. Optimal operational factors for nitrite accumulation in batch reactors. *Biodegradation* 12, 359–66.
- Bernet, N., Dangcong, P., Delgenès, J.-P., Moletta, R., 2001. Nitrification at Low Oxygen Concentration in Biofilm Reactor. *J. Environ. Eng.* 127, 266–271.
- Betlach, M.R., Tiedje, J.M., 1981. Kinetic explanation for accumulation of nitrite, nitric oxide, and nitrous oxide during bacterial denitrification. *Appl. Environ. Microbiol.* 42, 1074–1084.
- Blackburne, R., Yuan, Z., Keller, J., 2008. Partial nitrification to nitrite using low dissolved oxygen concentration as the main selection factor. *Biodegradation* 19, 303–312.
- Bower, C.E., Holm-Hansen, T., 1980. A Salicylate–Hypochlorite Method for Determining Ammonia in Seawater. *Can. J. Fish. Aquat. Sci.* 37, 794–798.
- Brockmann, D., Morgenroth, E., 2010. Evaluating operating conditions for outcompeting nitrite oxidizers and maintaining partial nitrification in biofilm systems using biofilm modeling and Monte Carlo filtering. *Water Res.* 44, 1995–2009.
- Burgess, J.E., Colliver, B.B., Stuetz, R.M., Stephenson, T., 2002. Dinitrogen oxide production by a mixed culture of nitrifying bacteria during ammonia shock loading and aeration failure. *J. Ind. Microbiol. Biotechnol.* 29, 309–313.
- Colliver, B.B., Stephenson, T., 2000. Production of nitrogen oxide and dinitrogen oxide by autotrophic nitrifiers. *Biotechnol. Adv.* 18, 219–232.
- Dalsgaard, T., Thamdrup, B., Farías, L., Revsbech, N.P., 2012. Anammox and denitrification in the oxygen minimum zone of the eastern South Pacific. *Limnol. Oceanogr.* 57, 1331–1346.
- Desloover, J., De Clippeleir, H., Boeckx, P., Du Laing, G., Colsen, J., Verstraete, W., Vlaeminck, S.E., 2011. Floc-based sequential partial nitrification and anammox at full scale with contrasting N₂O emissions. *Water Res.* 45, 2811–2821.
- Domingo-Félez, C., Mutlu, A.G., Jensen, M.M., Smets, B.F., 2014. Aeration strategies to mitigate nitrous oxide emissions from single-stage nitrification/anammox reactors. *Environ. Sci. Technol.* 48, 8679–8687.
- Domingo-Félez, C., Pellicer-Nàcher, C., Petersen, M.S., Jensen, M.M., Plósz, B.G., Smets, B.F., 2017. Heterotrophs are key contributors to nitrous oxide production in activated sludge under low C-to-N ratios during nitrification-Batch experiments and modeling. *Biotechnol. Bioeng.* 114, 132–140.
- Fux, C., Huang, D., Monti, A., Siegrist, H., 2004. Difficulties in maintaining long-term partial nitrification of ammonium-rich sludge digester liquids in a moving-bed biofilm reactor (MBBR). *Water Sci. Technol.* 49, 53–60.
- Füßel, J., Lam, P., Lavik, G., Jensen, M.M., Holtappels, M., Günter, M., Kuypers, M.M., 2012. Nitrite oxidation in the

- 527 Namibian oxygen minimum zone. *ISME J.* 6, 1200–1209.
- 528 Gao, K., Zhao, J., Ge, G., Ding, X., Wang, S., Li, X., Yu, Y., 2016. Effect of Ammonium Concentration on N₂O
529 Emission During Autotrophic Nitritation Under Oxygen-Limited Conditions. *Environ. Eng. Sci.* 0, 1–7.
- 530 Grasshoff, K., 1999. *Methods of Seawater Analysis*, 3rd ed. Wiley-VCH Verlag GmbH, Weinheim.
- 531 Guo, J., Peng, Y., Yang, X., Gao, C., Wang, S., 2013. Combination process of limited filamentous bulking and nitrogen
532 removal via nitrite for enhancing nitrogen removal and reducing aeration requirements. *Chemosphere* 91, 68–75.
- 533 Hellinga, C., Schellen, A.A.J.C., Mulder, J.W., Van Loosdrecht, M.C.M., Heijnen, J.J., 1998. The SHARON process:
534 An innovative method for nitrogen removal from ammonium-rich waste water. *Water Sci. Technol.* 37, 135–142.
- 535 Hiatt, W.C., Grady, C.P.L., 2008. An Updated Process Model for Carbon Oxidation, Nitrification, and Denitrification.
536 *Water Environ. Res.* 80, 2145–2156.
- 537 IPCC, 2013. *Climate Change 2013: The Physical Science Basis*, Cambridge University Press. Cambridge, United
538 Kingdom and New York, NY, USA.
- 539 Ishii, S., Song, Y., Rathnayake, L., Tumendelger, A., Satoh, H., Toyoda, S., Yoshida, N., Okabe, S., 2014.
540 Identification of key nitrous oxide production pathways in aerobic partial nitrifying granules. *Environ. Microbiol.*
541 16, 3168–3180.
- 542 Itokawa, H., Hanaki, K., Matsuo, T., 2001. Nitrous oxide production in high-loading biological nitrogen removal
543 process under low COD/N ratio condition. *Water Res.* 35, 657–664.
- 544 Jensen, M.M., Petersen, J., Dalsgaard, T., Thamdrup, B., 2009. Pathways, rates, and regulation of N₂ production in the
545 chemocline of an anoxic basin, Mariager Fjord, Denmark. *Mar. Chem.* 113, 102–113.
- 546 Kampschreur, M.J., Tan, N.C.G., Kleerebezem, R., Picioreanu, C., Jetten, M.S.M., Van Loosdrecht, M.C.M., 2008.
547 Effect of dynamic process conditions on nitrogen oxides emission from a nitrifying culture. *Environ. Sci. Technol.*
548 42, 429–435.
- 549 Kartal, B., Kuenen, J.G., van Loosdrecht, M.C.M., 2010. Sewage Treatment with Anammox. *Science* (80-.). 328, 702–
550 703.
- 551 Kim, S.W., Miyahara, M., Fushinobu, S., Wakagi, T., Shoun, H., 2010. Nitrous oxide emission from nitrifying activated
552 sludge dependent on denitrification by ammonia-oxidizing bacteria. *Bioresour. Technol.* 101, 3958–3963.
- 553 Kong, Q., Liang, S., Zhang, J., Xie, H., Miao, M., Tian, L., 2013. N₂O emission in a partial nitrification system:
554 Dynamic emission characteristics and the ammonium-oxidizing bacteria community. *Bioresour. Technol.* 127,
555 400–406.
- 556 Law, Y., Lant, P., Yuan, Z., 2013. The confounding effect of nitrite on N₂O production by an enriched ammonia-
557 oxidizing culture. *Environ. Sci. Technol.* 47, 7186–7194.
- 558 Law, Y., Lant, P., Yuan, Z., 2011. The effect of pH on N₂O production under aerobic conditions in a partial nitritation
559 system. *Water Res.* 45, 5934–5944.
- 560 Law, Y., Ye, L., Pan, Y., Yuan, Z., 2012. Nitrous oxide emissions from wastewater treatment processes. *Philos. Trans.*
561 *R. Soc. B Biol. Sci.* 367, 1265–1277.
- 562 Lemaire, R., Marcelino, M., Yuan, Z., 2008. Achieving the nitrite pathway using aeration phase length control and step-
563 feed in an SBR removing nutrients from abattoir wastewater. *Biotechnol. Bioeng.* 100, 1228–1236.
- 564 Liu, G., Wang, J., 2014. Role of Solids Retention Time on Complete Nitrification: Mechanistic Understanding and
565 Modeling. *J. Environ. Eng.* 140, 48–56.

- 566 Lv, Y., Ju, K., Wang, L., Chen, X., Miao, R., Zhang, X., 2016. Effect of pH on nitrous oxide production and emissions
567 from a partial nitrification reactor under oxygen-limited conditions. *Process Biochem.* 51, 765–771.
- 568 Mampaey, K.E., De Kreuk, M.K., van Dongen, U.G.J.M., van Loosdrecht, M.C.M., Volcke, E.I.P., 2016. Identifying
569 N₂O formation and emissions from a full-scale partial nitrification reactor. *Water Res.* 88, 575–585.
- 570 Mavrovas, I., 2014. “GraNiti SBR” Start-up and Operation of a Granular Nitrifying Sequencing Batch Reactor.
571 Technical University of Denmark.
- 572 McIlvin, M.R., Altabet, M.A., 2005. Chemical conversion of nitrate and nitrite to nitrous oxide for nitrogen and oxygen
573 isotopic analysis in freshwater and seawater. *Anal Chem* 77, 5589–5595.
- 574 Nielsen, L., 1992. Denitrification in sediment determined from nitrogen isotope pairing technique. *FEMS Microbiol.*
575 *Lett.* 86, 357–362.
- 576 Peng, L., Ni, B.-J., Ye, L., Yuan, Z., 2015. The combined effect of dissolved oxygen and nitrite on N₂O production by
577 ammonia oxidizing bacteria in an enriched nitrifying sludge. *Water Res.* 73, 29–36.
- 578 Peng, L., Ni, B.J., Erler, D., Ye, L., Yuan, Z., 2014. The effect of dissolved oxygen on N₂O production by ammonia-
579 oxidizing bacteria in an enriched nitrifying sludge. *Water Res.* 66, 12–21.
- 580 Poughon, L., Dussap, C.-G., Gros, J.-B., 2001. Energy model and metabolic flux analysis for autotrophic nitrifiers.
581 *Biotechnol. Bioeng.* 72, 416–433.
- 582 Rathnayake, R.M.L.D., Oshiki, M., Ishii, S., Segawa, T., Satoh, H., Okabe, S., 2015. Effects of dissolved oxygen and
583 pH on nitrous oxide production rates in autotrophic partial nitrification granules. *Bioresour. Technol.* 197, 15–22.
- 584 Rodriguez-Caballero, A., Pijuan, M., 2013. N₂O and NO emissions from a partial nitrification sequencing batch reactor:
585 Exploring dynamics, sources and minimization mechanisms. *Water Res.* 47, 3131–3140.
- 586 Schneider, Y., Beier, M., Rosenwinkel, K.-H., 2014. Influence of operating conditions on nitrous oxide formation
587 during nitrification and nitrification. *Environ. Sci. Pollut. Res. Int.* 21, 12099–12108.
- 588 Siegrist, H., Salzgeber, D., Eugster, J., Joss, A., 2008. Anammox brings WWTP closer to energy autarky due to
589 increased biogas production and reduced aeration energy for N-removal. *Water Sci. Technol.* 57, 383.
- 590 Sinha, B., Annachatre, A., 2007. Assessment of partial nitrification reactor performance through microbial population
591 shift using quinone profile, FISH and SEM. *Bioresour. Technol.* 98, 3602–3610.
- 592 Stein, L.Y., 2011. Surveying N₂O-Producing Pathways in Bacteria. *Methods Enzymol.* 486, 131–152.
- 593 Stokal, M., Kroeze, C., 2014. Nitrous oxide (N₂O) emissions from human waste in 1970–2050. *Curr. Opin. Environ.*
594 *Sustain.* 9–10, 108–121.
- 595 Tallec, G., Garnier, J., Billen, G., Gossailles, M., 2006. Nitrous oxide emissions from secondary activated sludge in
596 nitrifying conditions of urban wastewater treatment plants: Effect of oxygenation level. *Water Res.* 40, 2972–
597 2980.
- 598 Terada, A., Lackner, S., Kristensen, K., Smets, B.F., 2010. Inoculum effects on community composition and nitrification
599 performance of autotrophic nitrifying biofilm reactors with counter-diffusion geometry. *Environ. Microbiol.* 12,
600 2858–2872.
- 601 Terada, A., Sugawara, S., Hojo, K., Takeuchi, Y., Riya, S., Harper, W.F., Yamamoto, T., Kuroiwa, M., Isobe, K.,
602 Katsuyama, C., Suwa, Y., Koba, K., Hosomi, M., 2017. Hybrid Nitrous Oxide Production from a Partial
603 Nitrifying Bioreactor: Hydroxylamine Interactions with Nitrite. *Environ. Sci. Technol.* 51, 2748–2756.
- 604 Tokutomi, T., 2004. Operation of a nitrite-type airlift reactor at low DO concentration. *Water Sci. Technol.* 49, 81–88.

- Vadivelu, V.M., Keller, J., Yuan, Z., 2007. Free ammonia and free nitrous acid inhibition on the anabolic and catabolic processes of *Nitrosomonas* and *Nitrobacter*. *Water Sci. Technol.* 56, 89–97.
- van de Graaf, A.A., Bruijn, P. de, Robertson, L.A., Jetten, M.S.M., Kuenen, J.G., 1996. Autotrophic growth of anaerobic ammonium-oxidizing micro-organisms in a fluidized bed reactor. *Microbiology* 142, 2187–2196.
- van de Graaf, A.A. van de, Mulder, A., Bruijn, P. de, Jetten, M.S.M., Robertson, L.A., Kuenen, J.G., 1995. Anaerobic oxidation of ammonium is a biologically mediated process. *Appl. Environ. Microbiol.* 61, 1246–1251.
- Villaverde, S., Fdz-Polanco, F., García, P.A., 2000. Nitrifying biofilm acclimation to free ammonia in submerged biofilters. Start-up influence. *Water Res.* 34, 602–610.
- Wang, X.-H., Jiang, L.-X., Shi, Y.-J., Gao, M.-M., Yang, S., Wang, S.-G., 2012. Effects of step-feed on granulation processes and nitrogen removal performances of partial nitrifying granules. *Bioresour. Technol.* 123, 375–381.
- Warembourg, F.R., 1993. Nitrogen Fixation in Soil and Plant Systems, in: Knowles, R., Henry, B. (Eds.), *Nitrogen Isotope Techniques*. Academic Press, New York, pp. 127–155.
- Wett, B., Omari, A., Podmirseg, S.M., Han, M., Akintayo, O., Gómez Brandón, M., Murthy, S., Bott, C., Hell, M., Takács, I., Nyhuis, G., O’Shaughnessy, M., 2013. Going for mainstream deammonification from bench to full scale for maximized resource efficiency. *Water Sci. Technol.* 68, 283.
- Wiesmann, U., 1994. Biological nitrogen removal from wastewater. *Adv. Biochem. Eng. Biotechnol.* 51, 113–154.
- Wrage, N., Velthof, G.L., Van Beusichem, M.L., Oenema, O., 2001. Role of nitrifier denitrification in the production of nitrous oxide. *Soil Biol. Biochem.* 33, 1723–1732.
- Yamamoto, T., Takaki, K., Koyama, T., Furukawa, K., 2008. Long-term stability of partial nitrification of swine wastewater digester liquor and its subsequent treatment by Anammox. *Bioresour. Technol.* 99, 6419–6425.
- Yang, Q., Liu, X., Peng, C., Wang, S., Sun, H., Peng, Y., 2009. N₂O production during nitrogen removal via nitrite from domestic wastewater: Main sources and control method. *Environ. Sci. Technol.* 43, 9400–9406.
- Yang, Q., Peng, Y., Liu, X., Zeng, W., Mino, T., Satoh, H., 2007. Nitrogen Removal via Nitrite from Municipal Wastewater at Low Temperatures using Real-Time Control to Optimize Nitrifying Communities. *Environ. Sci. Technol.* 41, 8159–8164.
- Yang, S., Gao, M.M., Liang, S., Wang, S.G., Wang, X.H., 2013. Effects of step-feed on long-term performances and N₂O emissions of partial nitrifying granules. *Bioresour. Technol.* 143, 682–685.

Table 1. Overview of AOR, N₂OR and $\Delta\text{N}_2\text{O}/\Delta\text{NH}_4^+$ in R1 and R2 during phase 1 and 2. The net N₂O produced during each feed is stated as the percentage of total net N₂O production during the entire cycle.

	R1		R2	
	Phase 1 (Day 106–112)	Phase 2 (Day 395–451)	Phase 1 (Day 106–112)	Phase 2 (Day 397–463)
AOR (g N/L/d)	0.5 ± 0.05	0.60 ± 0.05	0.5 ± 0.02	0.76 ± 0.06
AOR (g N/g VSS/d)	1.04 ± 0.11	0.46 ± 0.09	1.78 ± 0.08	0.5 ± 0.02
N ₂ OR (mg N/g VSS/d)	5.9 ± 1.8	8.4 ± 3.5	16.0 ± 5.9	10.2 ± 3.5
$\Delta\text{N}_2\text{O}/\Delta\text{NH}_4^+$ (%)	0.6 ± 0.2	2.0 ± 1.0	0.8 ± 0.3	2.1 ± 0.7
Feed 1 (%)	23 ± 5	41 ± 9	30 ± 5	27 ± 5
Feed 2 (%)	22 ± 1	14 ± 2	21 ± 2	17 ± 2
Feed 3 (%)	19 ± 1	15 ± 2	18 ± 2	18 ± 2
Feed 4 (%)	17 ± 2	16 ± 2	16 ± 2	19 ± 1
Feed 5 (%)	18 ± 3	15 ± 4	15 ± 2	21 ± 5
# cycles	n=22	n=23	n=22	n=20

Table 2. Summary of net N₂O production rates during the ¹⁵N experiment (μg N/g VSS/min). Bulk N₂O production was based on liquid N₂O concentrations, measured with microsensors, while N₂O source partitioning is based on isotope additions

Days of operation	R1				R2			
	¹⁵ NO ₂ ⁻ additions				¹⁵ NO ₂ ⁻ additions			
	110		111		110		111	
	Feed 2	Feed 3	Feed 2	Feed 3	Feed 2	Feed 3	Feed 2	Feed 3
Bulk N ₂ O production rate	4.7	4.7	6.9	7.1	12	13	10	9.3
N ₂ O production rate from NO ₂ ⁻ (Eq. 3)	5.7	6.9	6.8	5.8	9.4	8.1	9.9	8.7
N ₂ O production from bulk NO ₂ ⁻ through ND (Eq. 4)	4.9	6.2	6.2	4.6	6.6	5.1	7.3	6.5
Total N ₂ O production through ND (Eq. 5)	6.7	7.6	7.4	7.4	13	13	13	11
Days of operation	¹⁵ NH ₄ ⁺ additions				¹⁵ NH ₄ ⁺ additions			
	106		107		106		107	
	Feed 2	Feed 3	Feed 2	Feed 3	Feed 2	Feed 3	Feed 2	Feed 3
	Feed 2	Feed 3	Feed 2	Feed 3	Feed 2	Feed 3	Feed 2	Feed 3
Bulk N ₂ O production rate	6.1	5.0	5.5	5.3	13	14	11	13
N ₂ O production from NH ₄ ⁺ (Eq. 3)	2.1	3.6	1.9	3.1	5.2	6.7	4.9	6.4
N ₂ O production via bulk NO ₂ ⁻	0.49	1.8	0.70	1.8	0.82	2.4	1.5	3.4
N ₂ O production not via bulk NO ₂ ⁻	1.6	1.8	1.2	1.3	4.4	4.3	3.4	3.0

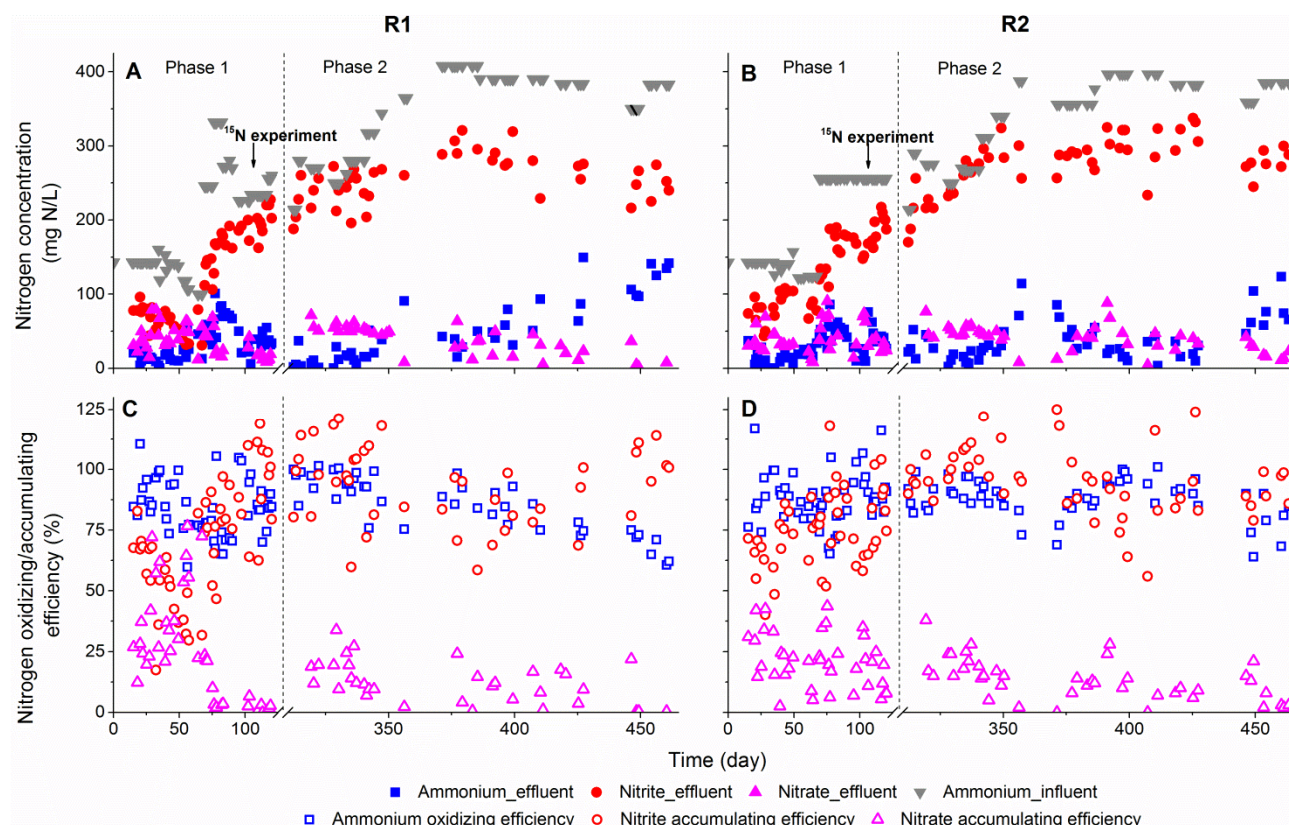


Fig. 1. Nitritation performance in R1 (A, C) and R2 (B, D) throughout the operational period. (A, B) Nitrogen concentrations (ammonium, nitrite and nitrate in effluent, ammonium in influent). (C, D) Nitrogen conversion efficiency (ammonium oxidizing efficiency (AOR/ALR), nitrite accumulation efficiency (NiAR/AOR), nitrate accumulation efficiency (NaAR/AOR)). The break at the X-axis represents a period of 170 days, when the reactors were stopped and biomass was stored at 4 °C.

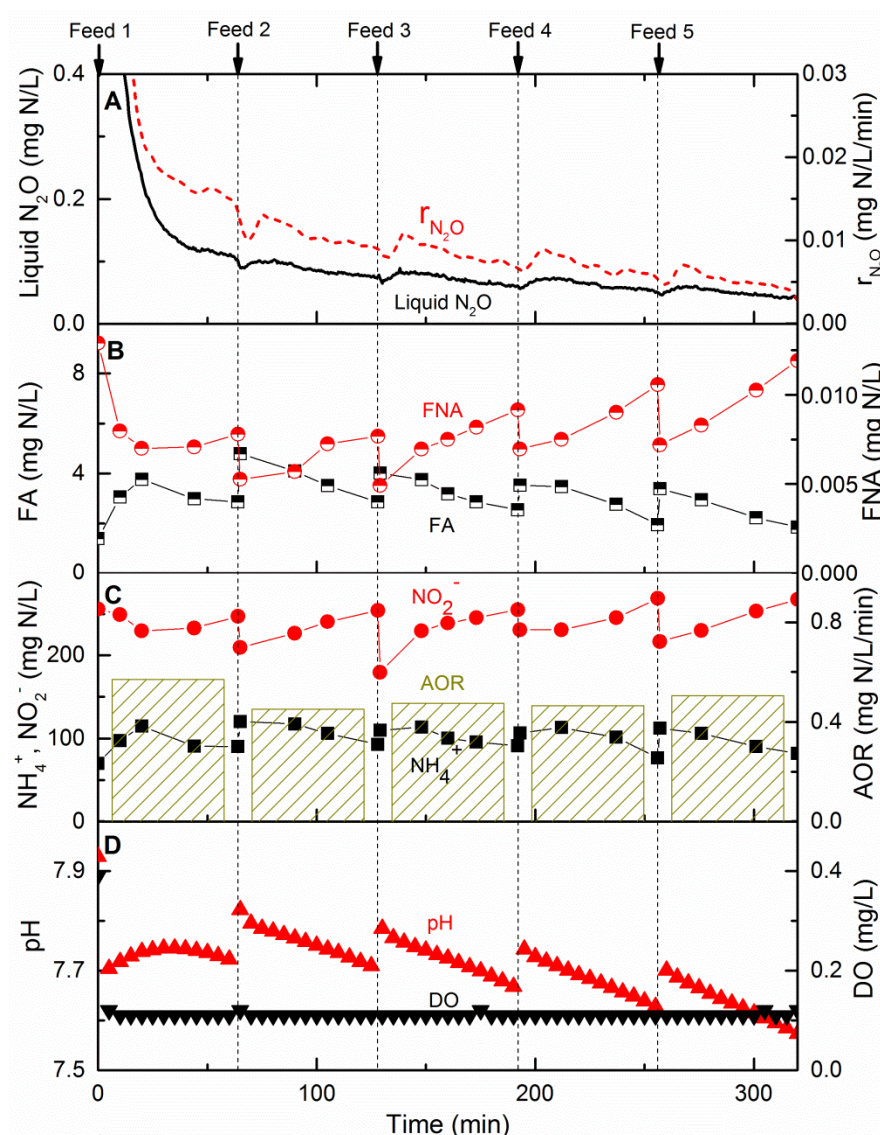


Fig. 2. In-cycle profiles of nitrogen species, pH, DO and N_2O in R1 (day 397). (A) Liquid N_2O concentrations and net N_2O production rates. (B, C) Bulk liquid nitrogen species (NO_2^- and NH_4^+), calculated free nitrous acid (FNA), free ammonia (FA) and ammonium oxidizing rates (AORs). (D) pH and DO.

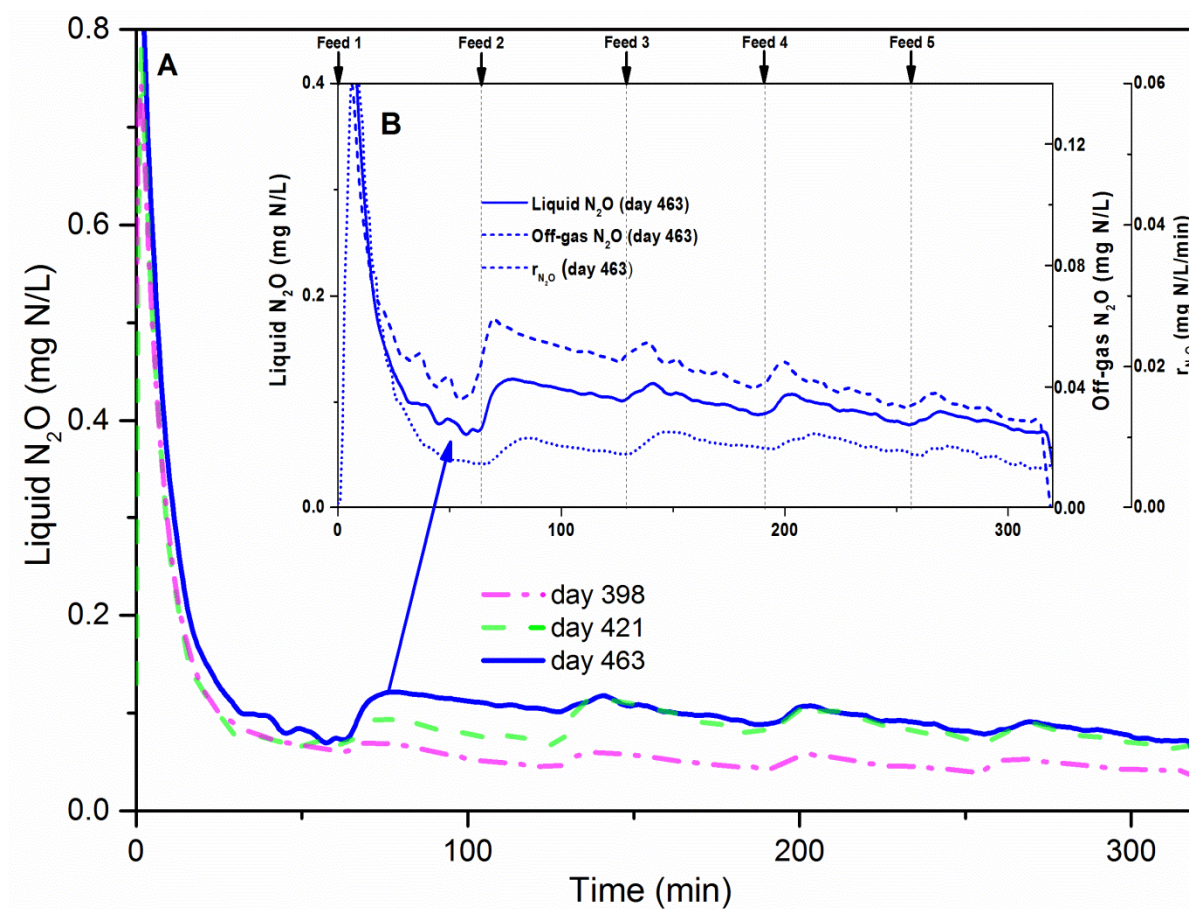


Fig. 3. (A) Profiles of liquid N_2O concentrations in one cycle in R2 on day 398, 421 and 463. (B) Profiles of liquid and off-gas N_2O concentrations and calculated net N_2O production rates in one cycle in R2 on day 463.

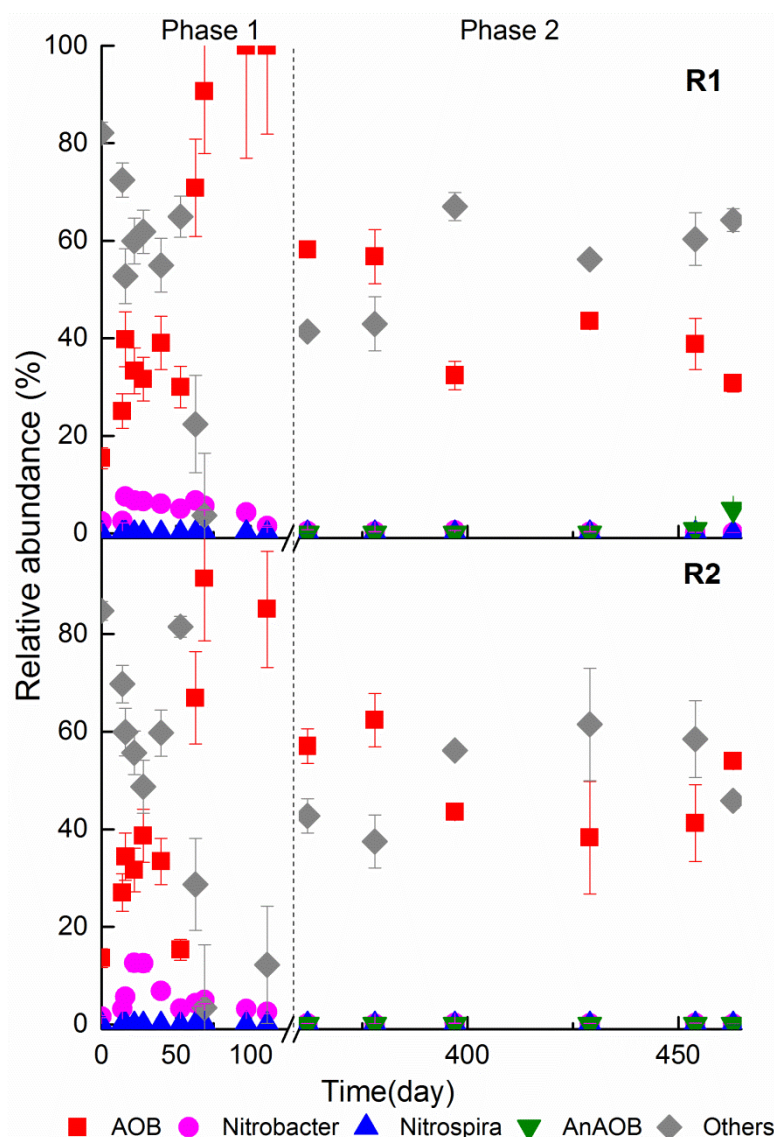


Fig. 4. Relative abundances of AOB, NOB, AnAOB and other bacteria in R1 and R2 over time based on qPCR of 16S rRNA genes. Error bars indicate standard deviations of duplicate measurements.

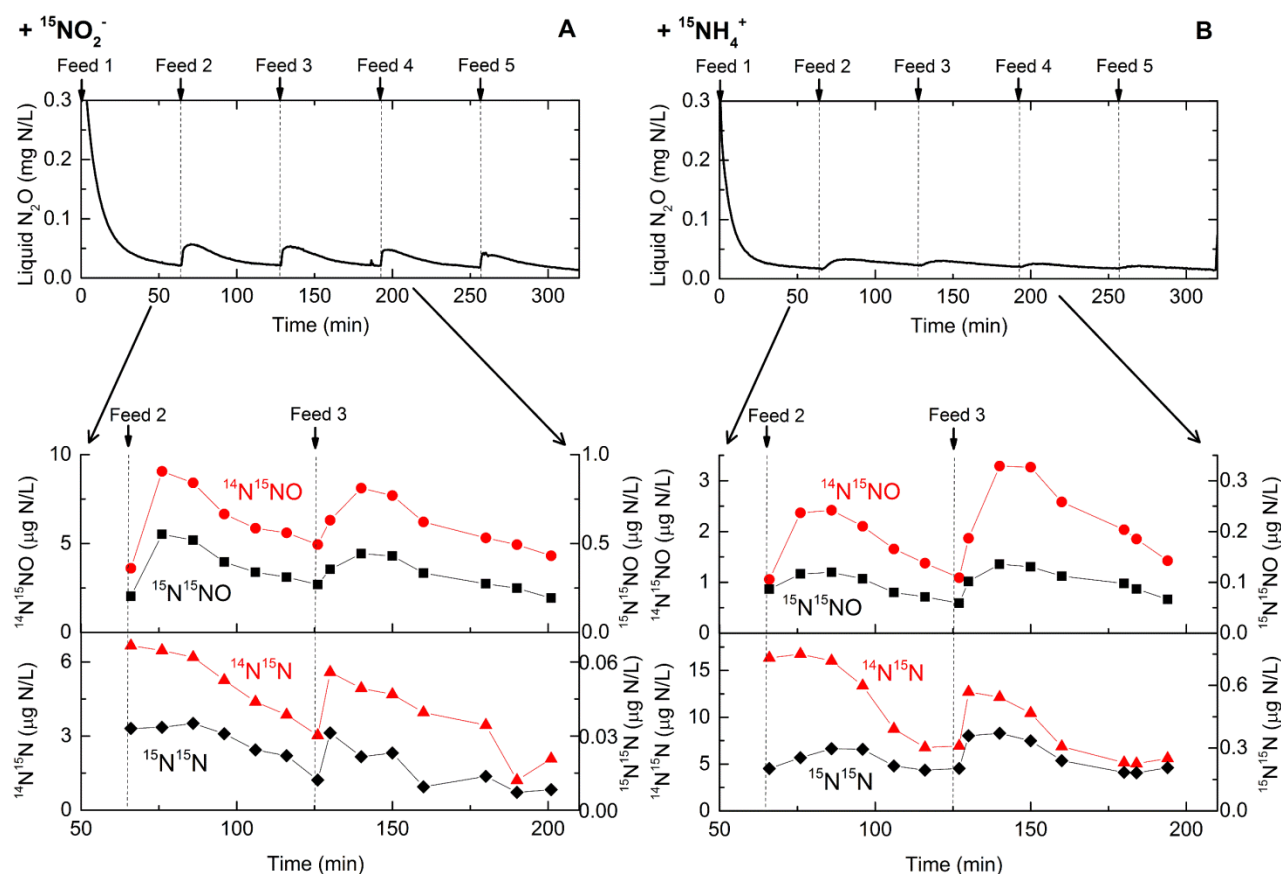


Fig. 5. Plots of bulk liquid N_2O concentrations versus time during the reaction phase of one cycle (upper panels) and isotopically labeled N_2O and N_2 concentrations versus time for feed 2 and 3 (lower panels) in Reactor 1. $^{15}\text{NO}_2^-$ spikes were performed at 111 days of operation (A) and $^{15}\text{NH}_4^+$ spikes at 107 days of operation (B).

Highlights

- Long-term high nitrification performance was achieved in intermittently-fed SBRs.
- Net N_2O production was, on average, 2.1% of the oxidized ammonium.
- Intermittent feeding appears an effective approach to mitigate N_2O emission.
- pH has a potential stimulatory effect on N_2O production.
- Nitrifier denitrification was the dominant source of N_2O production.